Carbonyl Insertion Reaction into the Pt—C Bond in Heterobimetallic $Pt(SnCl_3)(PH_3)_2(CO)(CH_3)$ Compound: Theoretical Study

WILLIAN R. ROCHA, WAGNER B. DE ALMEIDA

Laboratório de Química Computacional e Modelagem Molecular (LQC-MM), Departamento de Química, ICEx, UFMG, Belo Horizonte, MG, 31270-901, Brazil

Received 23 August 1999; accepted 14 January 2000

ABSTRACT: Quantum-mechanical calculations were carried out at the MP4(SDQ)//MP2 level of theory to determine the energies and reaction mechanism for the carbonyl insertion reaction (second step in the olefin hydroformylation catalytic cycle), using a heterobimetallic $Pt(SnCl_3)(PH_3)_2(CO)(CH_3)$ compound as a model catalytic species. The results show that this reaction proceeds through a three-center transition state, with an activation energy of 26.4 kcal/mol, followed by an intramolecular rearrangement to the square-planar *cis*-$Pt(SnCl_3)(PH_3)_2(MeCO)$ metal–acyl product. Analysis of the nature of the bonds shows that there is a negligible participation of the tin d-orbitals in the formation of the Pt—Sn bond. J Comput Chem 21: 668–674, 2000

Keywords: $Pt(SnCl_3)(PH_3)_2(CO)(CH_3)$; heterobimetallic; catalytic species; carbonyl insertion reaction; quantum mechanical

Correspondence to: W. B. De Almeida; e-mail: wagner@netuno.qui.ufmg.br

Contract/grant sponsor: Conselho Nacional de Desenvolvimento Científico e Tecnológico

Contract/grant sponsor: Fundação de Amparo à Pesquisa no Estado de Minas Gerais

Contract/grant sponsor: Science and Technology Ministry (MCT) of Brazil Programa de Apoio ao Desenvolvimento Científico e Tecnológico; contract/grant number: 62.0241/95.0

Introduction

The hydroformylation of olefins catalyzed by platinum complexes in combination with group 14 metal halides, forming the heterobimetallic catalytic system, is of great interest. As an example, catalyst precursors of the *cis*-$Pt(Cl)_2L_2$ type (L_2 = chiral or achiral phosphines), when combined with $SnCl_2$, have been shown to be highly active and selective in the hydroformylation of primary olefins,[1] and have recently been used in the synthesis of aldehydes and alcohols, relevant for the perfume industry, through the hydroformylation of naturally occurring terpenes.[2]

This Pt—Sn catalytic system has some advantages over the well-known and industrially used rhodium and cobalt catalysts, such as, for example, the low ratio of hydrogenation products generated in the hydroformylation.[2] However, some questions related to this system remain poorly understood. For example, the catalytic activity of this system is observed only in the presence of $SnCl_2$, suggesting that this cocatalyst plays a fundamental role in the entire catalytic cycle. Another complicating factor for the understanding of this heterobimetallic Pt—Sn system is the versatility of the $SnCl_2$, which can act in several different ways[1a]: (i) it may behave as a Lewis acid; (ii) it may act as a source of $SnCl_3^-$, which may act as a counterion; and (iii) it may act as ligand directly bound to platinum, favoring the insertion, carbonylation, and hydrogenolysis processes.

We recently engaged in the theoretical study of the Pt—Sn catalytic system, having investigated the formation of the cocatalyst, *trans*-$Pt(SnCl_3)(Cl)(PH_3)_2$, through the insertion reaction of $SnCl_2$ into the Pt—Cl bond in the *cis*-$Pt(Cl)_2(PH_3)_2$ compound,[3] and evaluated the energies and reaction mechanism for the olefin insertion reaction into the Pt—H bond (first step of the hydroformylation catalytic cycle), using the heterobimetallic *trans*-$Pt(H)(PH_3)_2(SnCl_3)$ compound as a model catalytic species, at the MP4(SDQ)//MP2 level of theory.[4] The next step in the hydroformylation catalytic cycle is the carbonylation of the metal–alkyl compounds, through the insertion of CO into the M—C bond. The carbonyl insertion reaction is one of the most important organometallic reactions, which appears in several catalytic cycles as one of the key steps,[5] and many experimental[6–8] and theoretical[9] studies have been carried out to understand this important reaction.

The main goal of the present work is to study, theoretically, the energetic and reaction mechanism for the carbonylation of the Pt—C bond using, as a model, the heterobimetallic $Pt(SnCl_3)(PH_3)_2(CO)(CH_3)$ compound. Because our model phosphine (PH_3) does not account for the rationalization of the steric effects along the reaction coordinate, we focus on the electronic effects of the ligands over the structure and chemical bonding along the reaction coordinate.

Computational Details

The geometry optimizations and frequency calculations have been carried out at the second-order Møller–Plesset perturbation (MP2) level of theory.[10] The relativistic effective core potential (ECP) and valence double-ξ basis set of Hay and Wadt (LANL2DZ)[11] was employed for the Pt and Sn atoms. This includes electrons in the 6s, 6p, and 5d orbitals for Pt and electrons in the 5s and 5p orbitals of Sn, described by the associated basis set of the form (3s3p3d)/[2s2p2d] and (3s3p)/[2s2p] for Pt and Sn, respectively. In addition, the valence basis set for the tin atom was augmented with a set of five d-polarization functions (α = 0.180).[12] For the P, C, and O atoms, the split-valence 6-31G[13] basis set was used. The spectator's Cl and H atoms were treated by a smaller split-valence 3-21G[13] basis set and minimal STO-3G[14] basis set, respectively. The transition state structures were located using the quadratic synchronous transit approach of Schlegel and coworkers,[15] starting with a low-level-computed Hessian matrix for a suitable guess transition state structure. Aiming to obtain better energetic results, single-point energy calculations on the MP2-optimized geometries were performed using fourth-order Møller–Plesset perturbation theory (MP4), with single, double, and quadruple excitations, called MP4(SDQ)//MP2.

All stationary points located on the potential energy surface were characterized as minima (no imaginary frequencies) or first-order transition state (characterized by having one imaginary frequency) through harmonic frequency calculations. To gain a deeper insight into the reaction pathway, we calculated the intrinsic reaction coordinate (IRC),[16] using the Gonzalez–Schlegel second-order path following,[17] starting from the optimized transition state structure, with a steplength of 0.100 $(\text{a.m.u.})^{1/2} \cdot$ bohr. The nature of the bonds in the molecules was analyzed with the natural bond orbital (NBO)[18] method of Weinhold and coworkers. All calculations reported here were carried out with the GAUSSIAN-94 package.

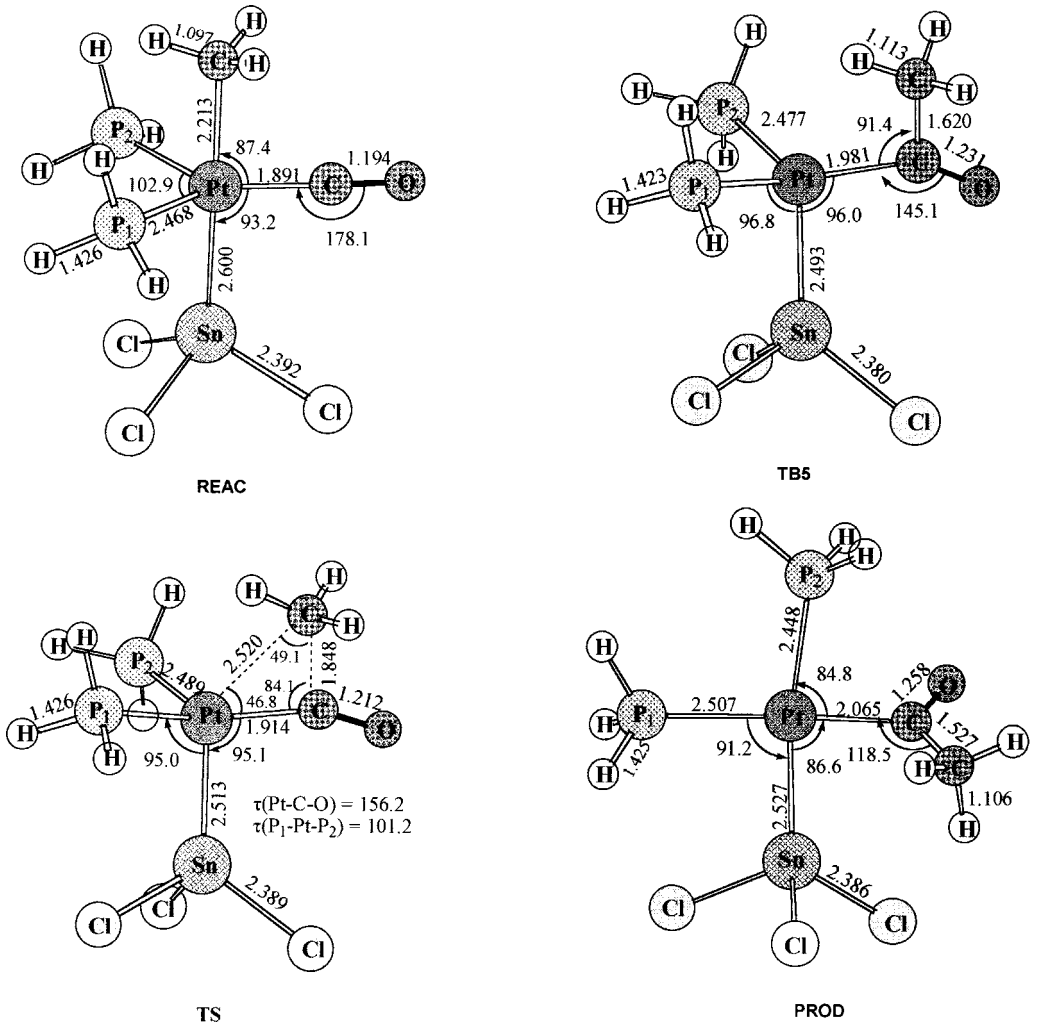

FIGURE 1. MP2-optimized structural parameters for the reactant (**REAC**) transition state (**TS**), intermediate (**TB5**), and product (**PROD**). Bond lengths are given in angstroms and bond angles in degrees.

Results and Discussion

REACTION MECHANISM

The MP2-optimized geometries for the reactant (**REAC**), transition state (**TS**), intermediate (**TB5**), and product (**PROD**) are shown in Figure 1. Figure 2 shows the MP2-calculated intrinsic reaction coordinate (IRC), and the variation of the main structural parameters along the reaction coordinate is shown in Figure 3.

The optimized reactant structure, **REAC** (Fig. 1), has a trigonal–bipyramidal structure, with the angles around the platinum coordination sphere slightly distorted from the expected optimal values for a trigonal–bipyramidal structure. The angles between the phosphine ligands are 102.9° and the

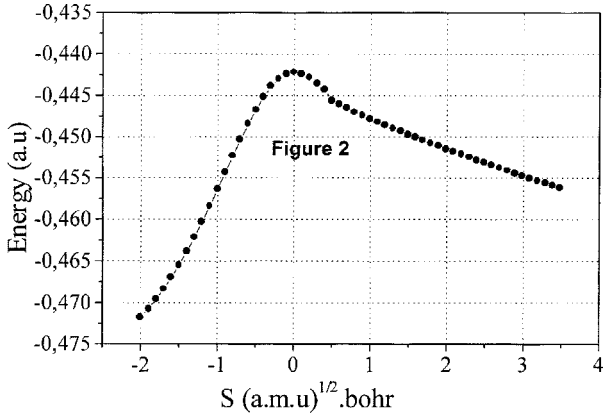

FIGURE 2. MP2-calculated intrinsic reaction coordinate (IRC) for the carbonyl insertion reaction. To obtain the total energy of a point *i* in the graph, the value −2331.000 should be added.

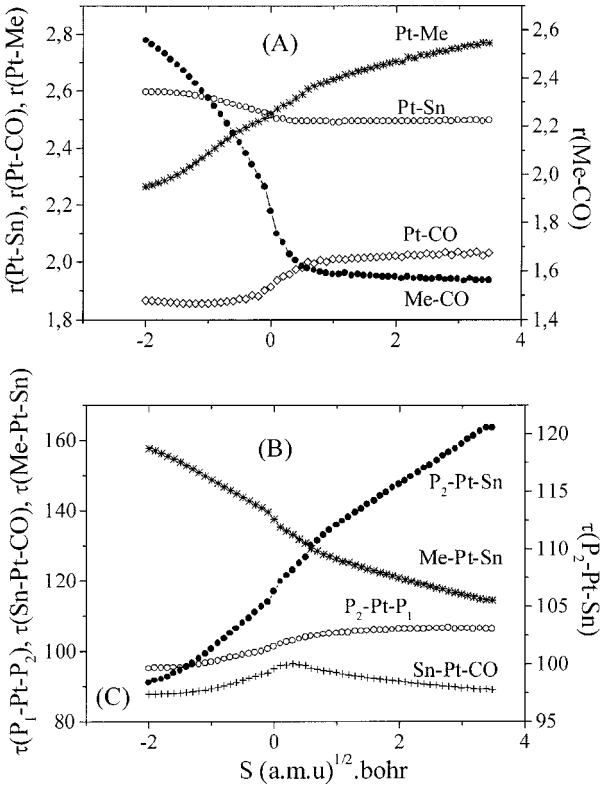

FIGURE 3. (A) Variation of the Pt—Me, Pt—Sn, Pt—CO, and Me—CO bond lengths along the reaction coordinate (given in angstroms). (B) Variation of the P_2—Pt—Sn, Me—Pt—Sn, P_2—Pt—P_1, and Sn—Pt—CO bond angles along the reaction coordinate (given in degrees).

angles between the phosphines and the CO ligand are 128.3°. The calculated Pt—Sn bond distance of 2.600 Å in **REAC** is in good agreement with the experimentally observed Pt—Sn bond length of 2.634 Å in *trans*-Pt(COPh)($SnCl_3$)(PEt_3)$_2$,[20] 2.601 Å in *trans*-Pt(H)($SnCl_3$)(PPh_3)$_2$,[21] and 2.600 Å in *trans*-Pt(H)($SnCl_3$)(Pcy_3)$_2$.[21] This compound then reacts, following a reaction mechanism given by the energetic profile shown in Figure 2. The variation of some bond lengths and bond angles along the reaction coordinate can be seen in Figure 3A and B, respectively. Until the reaction reaches the transition state, **TS**, a progressive migratory insertion of the CH_3 ligand into the Pt—CO bond takes place. Figure 3A shows the variation of bond lengths along the reaction coordinate. Analysis of Figure 3A shows that the Pt—Me and Me—CO bonds vary more appreciably than the other bonds, until reactant reaches the transition state. Pt—Me varies from 2.265 Å in $s = -2.0$ to 2.520 Å in **TS**, $s = 0.0$, and the Me—CO bond varies from 2.556 Å in $s = -2.0$, to 1.848 Å in **TS**. The other bond lengths change slowly, with Pt—CO starting to change when $s = -0.6$ and the Pt—Sn bond length is shortened, varying from 2.597 Å in $s = -2.0$ to 2.513 Å in **TS**. This shortening can be attributed to the fact that, as long as the CH_3 is transferred to the CO ligand, a vacant coordination site trans to the $SnCl_3$ moiety is created, and thus there will be more electron density over the Pt atom available to be donated to the $SnCl_3$ fragment, forming a stronger interaction. In other words, if the trans ligand is absent, the metal orbital becomes lower in energy and Sn can use more of the metal orbital(s) to strengthen the Pt—Sn bond. The movement of the methyl group toward the carbonyl ligand can be better seen in Figure 3B, by comparing the variation in the Sn—Pt—CH_3 and Sn—Pt—CO bond angles. The Sn—Pt—CH_3 starts with 180.6° in **REAC**, goes down to 157.7° in $s = -2.0$ and reaches 141.9° in **TS**, $s = 0.0$. At the same time, the Sn—Pt—CO bond remains almost constant (90.0°), between $s = -2.0$ and $s = -1.0$, and rises to 95.1° in **TS**. This means that the Sn—Pt—CO bond angle varies only 5° and, at the same time, the Sn—Pt—Me bond angle varies 38.7°, showing that this reaction does indeed occur with a migration of the alkyl group toward the CO ligand, which is in agreement with experimental findings.[6,7] The transition geometry that is reached, **TS** (see Fig. 1), is a three-center transition state, with an imaginary frequency of 330.0i cm^{-1}, in which the Pt—CH_3 bond is breaking and the Me—CO bond is forming. There is a substantial bending of the Pt—C—O bond, 156.2°, moving out of the linearity, which is consistent with the expected change in hybridization of the carbon atom when it moves from **REAC**, in which the carbon atom has sp hybridization, to **PROD**, where the carbon is sp^2hybridized. The detailed nature of these interactions are discussed in what follows. Once the transition state is reached, what takes place thereafter is a complete transfer of the CH_3 group to the CO ligand, from $s = 0.0$ to $s = 0.5$, forming a metal–acyl intermediate. The structure corresponding to this point, $s = 0.5$, is shown in Figure 1, with the label **TB5**. This structure also has a trigonal–bipyramidal-like structure, with a vacant coordination site trans to the $SnCl_3$ moiety. We performed a MP2 vibrational frequency analysis at this geometry, **TB5**, to assess the nature of this point,[22] and verified that this structure is not indeed a true minimum, rather it has a very small imaginary frequency of 57.6i cm^{-1}, corresponding to the rotation of the PH_3 ligand. After $s = 0.5$, what happens is a slow intramolecular rearrangement from the trigonal–bipyramidal structure **TB5** to the

TABLE I.
Calculated Total Energies, E_{tot} (a.u.), Zero-Point Energies, ZPE (kcal/mol), Relative Energies, E_{rel} (kcal/mol), and Gibbs Free Energy Differences, ΔG (kcal/mol).

	MP2				MP4(SDQ)//MP2[a]	
	E_{tot}	ZPE	E_{rel}[b]	ΔG	E_{tot}	E_{rel}
REAC	−2331.488928	66.5	0	0	−2331.551658	0
TS[c]	−2331.442169	65.2	29.3 (28.0)	28.1	−2331.507523	27.7 (26.4)
PROD	−2331.476969	67.1	7.5 (8.1)	8.0	−2331.549612	1.3 (1.9)

[a] Single-point energy calculation on the MP2-optimized geometry.
[b] Values in parentheses were obtained with ZPE corrections calculated at the MP2 level.
[c] Imaginary frequency: 330.0i cm^{-1}.

square-planar product, **PROD**. As can be seen in Figure 3A, all bond distances remain constant (except the Pt—Me bond), and the other angular variables act more effectively, as shown in Figure 3B. The P_2—Pt—Sn bond angle is opened, ranging from 109.3° in **TB5**, $s = 0.5$, to 171.2° in the square-planar product, **PROD**. The angle between the phosphines varies from 101.2° in $s = 0.5$ to 97.4° in **PROD**, and the Pt—C—O bond angle changes from 145.1° in **TB5** to 119.1° in **PROD**. This reasoning is illustrated in Figure 3B.

BONDING AND REACTION ENERGETICS

The total and relative energies, and some thermodynamical quantities for this carbonyl insertion reaction are listed in Table I. As can be seen, the reaction proceeds with an activation energy of 28.0 kcal/mol at the MP2 level of theory, with ZPE corrections included, and 26.4 kcal/mol at the MP4(SDQ)//MP2 level. The activation energy for the carbonyl insertion reaction, with the industrially used catalyst of rhodium and cobalt, has already been evaluated with the help of theoretical methodologies, and it is of interesting to compare these results with our values. Morokuma and coworkers[9e] studied the carbonyl insertion reaction in the $Rh(PH_3)_2(CO)_2(Et)$ compound and found that, at the MP2 evel of theory, >20 kcal/mol is required for this reaction to take place. Ziegler and coworkers[9g] calculated the activation energy for the CO insertion in $(CH_3)Co(CO)_4$, using the density functional level of theory, and obtained an activation energy barrier for the direct process of the order of 20 kcal/mol and an activation energy for the inverse process (decarbonylation) of only 2.2 kcal/mol. Therefore, the activation energy for the carbonylation step, using the Pt—Sn catalyst, is of almost the same magnitude as that found for the rhodium and cobalt catalyst. The calculated Gibbs free energy of activation, ΔG^*, is 28.1 kcal/mol, which is practically the same as the MP2 activation energy of 28.0 kcal/mol. The reaction proceeds with an endothermicity of 8.1 kcal/mol at the MP2 level of theory, but when MP4(SDQ) single-point energy calculation is performed we observe a drastic reduction to 1.9 kcal/mol, as it can be seen in Table I.

Table II shows the NBO analysis of the Pt—Sn and Pt—CO bonding orbitals obtained with the MP2 wave function. As can be seen, in the reactant, **REAC**, the Pt—Sn bonding orbital is not polarized toward any of the atoms. The polarization coefficient of the Pt and Sn atoms are 0.714 and 0.700, respectively, showing that this bond orbital is composed of 50% Pt and 49.5% Sn. This orbital is formed through the interaction of a $sd^{1.09}$ hybrid on the platinum atom, composed by the mixing of the 6s, $5d_{x2-y2}$ and $5d_{z2}$ atomic orbitals, with an $sp^{1.18}$ hybrid on Sn, composed by the combination of the 5s, $5p_x$, and $5p_y$ atomic orbitals. The Pt—CO bonding orbital in **REAC** is formed through the interaction of a $sd^{1.02}$ hybrid on Pt, composed of the 6s, $5d_{x2-y2}$, and $5d_{z2}$ atomic orbitals, with an $sp^{0.59}$ hybrid on the carbon atom. The polarization coefficient for this Pt—CO bonding orbital of 0.503 on Pt and 0.864 on C shows that it is polarized toward the carbon atom. In the transition state, **TS**, the bonding situation is slightly different. The polarization coefficient of 0.678 on the platinum atom and 0.735 on the Sn atom shows that this bond is now polarized toward the tin atom, which, as noted before, can be explained by the fact that, in **TS**, there is a vacant coordination site trans to the $SnCl_3$ ligand, which allows the $SnCl_3$ to drawn back electron density from the Pt atom. This Pt—Sn bonding orbital in **TS** is formed through the interaction of a $sd^{0.59}$ hybrid on Pt, formed by mixing of the 6s, $5d_{x2-y2}$, and $5d_{z2}$

TABLE II.
Natural Bond Orbitals Analysis Using the MP2 Wave Function.[a]

Bond Orbital	REAC	TS	PROD
σ (Pt—Sn)	$0.714(sd^{1.09})Pt + 0.700(sp^{1.18})Sn$	$0.678(sd^{0.59})Pt + 0.735(sp^{1.77})Sn$	$0.687(sd^{0.63})Pt + 0.726(sp^{1.68})Sn$
h_{Pt}	$0.688(6s) + 0.658(5d_{x2-y2}) - 0.257(5d_{z2})$	$0.784(6s) + 0.561(5d_{x2-y2}) + 0.101(5d_{z2})$	$0.780(6s) + 0.613(5d_{x2-y2})$
h_{Sn}	$0.611(5s) + 0.782(5p_x) + 0.111(5p_y)$	$0.599(6s) + 0.791(5p_x) - 0.106(5p_y)$	$0.610(5s) + 0.787(5p_x)$
σ (Pt—CO)	$0.503(sd^{1.02})Pt + 0.864(sp^{0.59})C$	$0.830(sd^{1.83})Pt + 0.558(sp^{1.82})C$	$0.680(sd^{1.85})Pt + 0.733(sp^{2.59})$
h_{Pt}	$-0.703(6s) + 0.690(5d_{x2-y2}) - 0.118(5d_{z2})$	$-0.593(6s) + 0.757(5d_{x2-y2}) + 0.189(5d_{z2})$	$-0.592(6s) + 0.762(5d_{x2-y2}) + 0.237(5d_{z2})$
h_C	$-0.792(2s) + 0.609(2p_y)$	$-0.576(2s) + 0.452(2p_y) - 0.181(2p_z)$	$-0.526(2s) - 0.847(2p_y)$

[a] h_{Pt}, h_{Sn}, and h_C are decomposition of the hybrids on the Pt, Sn, and C atoms, respectively, which participates in the bond.

SCHEME 1.

atomic orbitals, with an $sp^{1.77}$ hybrid on tin, formed by the 6s, $5p_x$, and $5p_y$ atomic orbitals. In **TS** we also observe an inversion of the polarity of the Pt—CO bond as compared with the Pt—CO bond in **REAC**, as can be seen by the polarization coefficient of 0.830 on Pt and 0.558 on carbon, and as compared with 0.503 and 0.864 on Pt and C, respectively, in **REAC**. Scheme 1 shows the three-center interaction in **TS** (obtained using the 3CBOND option of the NBO program implemented in the GAUSSIAN package).

In the square-planar product, **PROD**, the polarity of the Pt—Sn bonding orbital toward the Sn atom is maintained as in **TS**, as can be seen by the polarization coefficient of 0.726 on Sn and 0.687 on Pt. This orbital is now formed by the interaction of an $sd^{0.63}$ hybrid over Pt, formed by mixing of the 6s and $5d_{x2-y2}$ atomic orbitals, with an $sp^{1.68}$ hybrid on tin. The Pt—CO bonding orbital is formed through the interaction of an $sd^{1.85}$ hybrid on Pt with a $sp^{2.59}$ hybrid on the carbon atom. It is important note that the participation of the d-orbitals on the tin atom in forming the Pt—Sn bond is negligible. The percentages of Sn d-orbital in the Pt—Sn bond are 0.29%, 0.47%, and 0.47% in **REAC**, **TS**, and **PROD**, respectively, which is in apparent disagreement with the assumption that the Sn atom can make a d–d back-donation type of interaction with the Pt atom.[23] As seen in Table II, it seems that this type of interaction is probably of the d–p-type.

Summary and Conclusions

In this work, we evaluated the energies and reaction mechanism of the carbonyl insertion reaction into the Pt—C bond (the second step of the olefin hydroformylation catalytic cycle), at the

MP4(SDQ)//MP2 level of theory, using a heterobimetallic $Pt(SnCl_3)(PH_3)_2(CO)(CH_3)$ compound as a model catalytic species. All stationary points located on the potential energy surface were fully optimized and characterized through harmonic frequency analysis. The reaction proceeds through a three-center transition state with a trigonal–bipyramidal-like structure. The intrinsic reaction coordinate calculations showed that this reaction occurs with a progressive migratory insertion of the methyl group into the Pt—CO bond, followed by an intramolecular rearrangement to generate the square-planar *cis*-$Pt(SnCl_3)(PH_3)_2(MeCO)$ metal–acyl product. This carbonyl insertion reaction proceeds with activation energy of 28.0 kcal/mol and an endothermicity of 8.0 kcal/mol, as evaluated at the MP2 level of theory. However, when MP4(SDQ) single-point energy calculations are performed, the activation energy is reduced to 26.4 kcal/mol, and the reaction endothermicity is drastically reduced to 1.9 kcal/mol. We also performed NBO analysis of the Pt—Sn and Pt—CO bonding orbitals in the reactant, transition state, and product, which showed that the participation of d-orbitals on the tin atom is negligible when forming the Pt—Sn bond.

Acknowledgments

This work could not be have been done without the computer resources of the CENAPAD-MG/CO (Centro Nacional de Processamento de Alto Desempenho, Região Centro-Oeste). We also thank Prof. E. V. Gusevskaya and Prof. E. N. Dos Santos for kindly providing reprints of their recent experimental studies.

References

1. (a) Scrivanti, A.; Benton, A.; Toniolo, L.; Botteghi, C. J Organomet Chem 1986, 314, 369; (b) Parrinelo, G.; Stille, J. K. J Am Chem Soc 1987, 109, 7122; (c) Kóllar, L.; Consiglio, G.; Pino, P. J Organomet Chem 1987, 330, 305; (d) Botteghi, C.; Marchetti, M.; Del Ponte, G. Quim Nova 1992, 15, 21; (e) Botteghi, C.; Marchetti, M.; Del Ponte, G. Quim Nova 1997, 20, 30; (f) Gómez, M.; Muller, G.; Sainz, D.; Sales, J. Organometallics 1991, 10, 4036.
2. (a) Augusti, R.; Gusevskaya, E. V.; Dos Santos, E. N.; Teles, W. M.; Filgueiras, C. A. L. Proceedings of Eighth Sminário Brasileiro de Catálise, Nova Friburgo, RJ, Brazil, 1995, Vol. 1, pp. 360–367; (b) Gusevskaya, E. V.; Gonçalves, J. A. J Mol Catal 1997, 121, 131; (c) Dias, A. O.; Augusti, R.; Dos Santos, E. N.; Gusevskaya, E. V. Tetrahedron Lett 1997, 38, 41; (d) Da Rocha, L. L.; Dias, A. O.; Dos Santos, E. N.; Gusevskaya, E. V. J Mol Catal A Chem 1998, 132, 213.
3. Rocha, W. R.; De Almeida, W. B. Int J Quantum Chem 1997, 65, 643.
4. Rocha, W. R.; De Almeida, W. B. Organometallics 1998, 17, 1961.
5. (a) Yamamoto, A. Organotransition Metal Chemistry: Fundamental Concepts and Applications; Wiley: New York, 1986; (b) Gates, B. C. Catalytic Chemistry; Wiley: New York, 1992.
6. (a) Noack, K.; Calderazzo, F. J Organomet Chem 1967, 10, 101; (b) Calderazzo, F. Angew Chem Int Ed Engl 1977, 16, 299.
7. (a) Anderson, G. K.; Cross, R. J. J Chem Soc Dalton Trans 1979, 1246; (b) Anderson, G. K.; Cross, R. J. Acc Chem Res 1984, 17, 67.
8. Ozawa, F.; Yamamoto, A. Chem Lett 1981, 289.
9. (a) Sakaki, S.; Kitaura, K.; Morokuma, K.; Ohkubo, K. J Am Chem Soc 1983, 105, 2280; (b) Koga, N.; Morokuma, K. J Am Chem Soc 1985, 107, 7230; (c) Koga, N.; Morokuma, K. J Am Chem Soc 1986, 108, 6136; (d) Koga, N.; Morokuma, K. New J Chem 1991, 15, 749; (e) Matsubara, T.; Koga, N.; Ding, Y.; Musaev, D. G.; Morokuma, K. Organometallics 1997, 16, 1065; (f) Ziegler, T.; Versluis, L.; Tschinke, V. J Am Chem Soc 1986, 108, 612; (g) Versluis, L.; Ziegler, T. J Am Chem Soc 1989, 111, 2018.
10. Møller, C.; Plesset, M. S. Phys Rev 1934, 46, 618.
11. Hay, P. J.; Wadt, W. R. J Chem Phys 1985, 82, 270.
12. Höllwarth, A.; Böhme, M.; Dapprich, S.; Ehlers, A. W.; Gobbi, A.; Jonas, V.; Köhler, K. F.; Stegmann, R.; Veldkamp, A.; Frenking, G. Chem Phys Lett 1993, 208, 237.
13. Hehre, W. J.; Ditchfield, R.; Pople, J. A. J Chem Phys 1972, 56, 2257.
14. Hehre, W. J.; Stewart, R. F.; Pople, J. A. J Chem Phys 1969, 51, 2657.
15. Peng, C.; Schlegel, H. B. Israel J Chem 1993, 33, 449.
16. Fukui, K. Acc Chem Res 1981, 14, 363.
17. (a) Gonzalez, C.; Schlegel, H. B. J Chem Phys 1989, 90, 2154; (b) Gonzalez, C.; Schlegel, H. B. J Phys Chem 1990, 94, 5523.
18. Reed, A. E.; Curtis, L. A.; Weinhold, F. Chem Rev 1988, 88, 899.
19. Frisch, M. J.; Trucks, G. W.; Schlegel, H. B.; Gill, P. M. W.; Johnson, B. G.; Robb, M. A.; Cheeseman, J. R.; Keith, T. A.; Peterson, G. A.; Montgomery, J. A.; Raghavachari, K.; Al-Lahan, M. A.; Zakrzewski, V. G.; Ortiz, J. V.; Foresman, J. B.; Cioslowski, J.; Stefanov, B. B.; Nanayakkara, A.; Challacombe, M.; Peng, C. Y.; Ayala, P. Y.; Chen, W.; Wong, M. W.; Andres, J. L.; Replogle, E. S.; Gomperts, R.; Martin, R. L.; Fox, D. J.; Binkley, J. S.; Defrees, D. J.; Baker, J.; Stewart, J. P.; Head-Gordon, M.; Gonzalez, C.; Pople, J. A. GAUSSIAN-94 (revision A.1), Gaussian, Inc., Pittsburgh, PA, 1995.
20. Albinati, A.; Gunten, U. N.; Pregosin, P. S.; Ruegg, H. J. J Organomet Chem 1985, 295, 239.
21. Goméz, M.; Muller, G.; Sainz, D.; Sales, J. Organometallics 1991, 10, 4036.
22. When the IRC calculation reached **TB5** point convergence instability was observed. This is due to the fact that this point is not a minimum on the IRC reaction path, although it is a true stationary point. We have not looked at a bifurcation point on the PES; however, we agree that it might be there.
23. Pettit, L. D. Q Rev 1972, 56, 2257.